J Exp Biol Advance Online Articles. First posted online on 27 February 2014 as doi:10.1242/jeb.085522
Access the most recent version at http://jeb.biologists.org/lookup/doi/10.1242/jeb.085522

Load-induced changes in bone stiffness and cancellous and cortical bone mass following tibial compression diminish with age in female mice

Russell P. Main[1*], Maureen E. Lynch[1+], Marjolein C.H. van der Meulen[1,2]

1. Sibley School of Mechanical and Aerospace Engineering, Cornell University, Ithaca, NY 14853 USA

2. Laboratory for Biomedical Mechanics and Materials, Hospital for Special Surgery, New York, NY 10021 USA

*Present address: Department of Basic Medical Sciences, College of Veterinary Medicine and Weldon School of Biomedical Engineering, Purdue University, West Lafayette, IN 47907 USA
+ Present address: Department of Biomedical Engineering, Cornell University, Ithaca, NY 14853 USA

Short title: Tibial adaptation in growing female mice
Keywords: bone, tibia, cancellous, cortical, stiffness, mouse, load

Corresponding author:
Russell P. Main, Ph.D.
Department of Basic Medical Sciences
College of Veterinary Medicine
Purdue University
625 Harrison Street
West Lafayette, IN 47907 USA
phone: 765.494.0898
fax: 765.494.0781
e-mail: rmain@purdue.edu

Summary: 250/250 words
# of words (Introduction through Funding): 5,532 words
# of tables: 2
# of figures: 7

Summary

The vertebrate skeleton is an adaptive structure that responds to mechanical stimuli by increasing bone mass under increased mechanical loads. Although experimental animal models have shown the anabolic cortical bone response to applied load decreases with age, no consensus exists regarding whether this adaptive mechanism is affected by age in cancellous bone, the tissue most impacted by age-related bone loss. We used an established murine in vivo tibial loading model to characterize the load-induced cancellous, cortical, and whole bone responses to mechanical stimuli in growing and mature female mice at 6, 10, and 16wks of age. The effects of applied load on tibial morphology and stiffness were determined using microcomputed tomography and in vivo bone strains measured at the medial tibial midshaft during applied loading. At all ages, two weeks of applied load produced larger midshaft cortical cross-sectional properties (+13-72%) and greater cancellous bone volume (+21-107%) and thicker trabeculae (+31-68%) in the proximal metaphyses of the loaded tibiae. The relative anabolic response decreased from 6wks to 16wks of age in both the cancellous and cortical envelopes. Load-induced tibial stresses decreased more in 6wk old mice following loading, which corresponded to increased in vivo tibial stiffness. Stiffness in the loaded tibiae of 16wk old mice decreased despite moderately increased cortical cross-sectional geometry, suggesting load-induced changes in bone material properties. This study shows that the cancellous and cortical anabolic responses to mechanical stimuli decline with age into adulthood and that cortical cross-sectional geometry alone does not necessarily predict whole bone functional stiffness.

Introduction

The vertebrate skeleton is an adaptive structure that remodels to meet physiological and physical demands. Mechanical forces are important influences on skeletal growth and remodeling, due to the skeleton's role in structural support. Racquet sport athletes provide an excellent example of the anabolic effects of mechanical loading on the skeleton, as bones in their dominant playing arms are larger than their non-dominant arms (Jones et al., 1977; Ruff et al., 1994; Kannus et al., 1995; Haapsalo et al., 1998; Bass et al., 2002). By contrast, bone mass in the long bones of astronauts, paralytics, and patients on long-term bedrest decreases following the removal of normal functional loads on the skeleton (Lang et al., 2004; Sievanen, 2010). Thus, modeling and remodeling in the skeleton serve to increase skeletal mass to withstand increased habitual loads while also preventing an unnecessarily robust skeleton that would be metabolically costly to support relative to the mechanical forces experienced.

In vivo loading models are commonly used to understand the regulation of bone cell function and skeletal structure by mechanical stimuli. Through these models, we know that the anabolic response of cortical bone to mechanical stimuli is greater in growing animals than in adults (Rubin et al., 1992; Turner et al., 1995; Srinivasan et al., 2003; Lynch et al., 2011). Similar age-related skeletal decreases in the response to exercise have been reported in humans (Kannus et al., 1995; Bass et al., 2002). Although the age-dependent cortical response to mechanical stimuli is well documented, understanding the response of cancellous tissue architecture and bone mass to physical stimuli with age is of key importance because corticocancellous sites in the skeleton, such as the femoral head, vertebrae, and distal radius, are most susceptible to osteoporotic fracture (Melton et al., 2003). Developing a clear understanding of age-related changes in the whole bone response to mechanical stimuli, including both cortical

and cancellous tissues, will enable future research to focus on characterizing specific cellular mechanisms regulating anabolic processes in the skeleton.

Histomorphometric and radiological measures are the current standard to assess the skeletal response to applied load in in vivo models (Rubin et al., 1992; Robling et al., 2001; Gross et al., 2002; Fritton et al., 2005; de Souza et al., 2005). However, these techniques do not directly reflect whole bone function during loading. Restricting post-loading assessments of the skeletal response to load to only the cortical and cancellous envelopes does not account for load-induced changes in whole bone morphology that can have important consequences for whole bone mechanical adaptation to applied load. For example, longitudinal bone curvature affects the moments acting on the skeleton and load transmission through the limb (Biewener, 1983b; Lanyon, 1987; Main et al., 2010; Dodge et al., 2012) and is sensitive to physical stimuli, decreasing in response to both removal or application of mechanical loads (Lanyon, 1980; Biewener and Bertram, 1994; Mosley et al., 1997). Similarly, ex vivo mechanical tests incorporating strain gauge measures are rarely used to determine changes in whole bone mechanical behaviour following loading. Studies that have incorporated these measures examined partially dissected limbs in euthanized rodents (Robling et al., 2002, Warden et al., 2005). However, both euthanasia and dissection of the surrounding tissues could significantly influence strain gauge-based stiffness measures (Dodge et al., 2012). No studies to date have examined functional alterations in whole bone stiffness by measuring bone strains on the intact limbs of living rodents following adaptation to in vivo mechanical loading. Absence of these measures is significant given the load-bearing function of the skeleton and the hypothesized importance of tissue strains in modulating bone's biological response to load (Carter, 1982; Frost, 1983; Lanyon, 1987). Thus, measuring in vivo bone stiffness in relation to changes in

whole bone morphology following controlled applied loading is a critical next step in developing anabolic loading therapies for the skeleton.

In this study, we examine changes in the skeleton's structural response to applied load in three age groups of female mice ranging from young, growing animals to mature adults. This ontogenetic approach provides developmental context for the discrepancies found in previous studies for the corticocancellous response to applied load and complements our previous work showing that the skeletal response to mechanical strain was similar in 10wk old male and female mice and significantly reduced in mature 26wk old female mice (Lynch et al., 2010; Lynch et al., 2011). The goals of this study were to determine (1) cancellous and cortical adaptation to applied load in growing and adult female mice as a function of age and (2) the contribution of age-dependent changes in cortical and whole bone morphological adaptation to bone stiffness. To address these goals, an established osteogenic loading protocol was applied to the tibiae of growing and adult female C57Bl/6 mice (6, 10, and 16wks old)(Fig. 1). We hypothesized that bone mass will increase in the loaded tibiae, but that the anabolic response to loading will decrease with age in cancellous and cortical bone of growing and adult female mice. Secondly, stiffness in the loaded tibiae will be greater than in the non-loaded control tibiae due primarily to load-induced increases in cortical bone geometry and decreases in longitudinal bone curvature.

Results

Applied load had a significant anabolic effect on cancellous tissue mass in the proximal tibial metaphysis, and the relative effect of load decreased with age (Figs. 2, 3; Table 1). Cancellous bone volume fraction (BV/TV) was 107%, 60%, and 21% greater in the loaded relative to the control tibiae in the 6wk, 10wk, and 16wk old mice, respectively (Fig. 3).

Similarly, trabecular thickness (Tb.Th) was 68%, 42%, and 31% greater in the loaded relative to the control limbs in the 6wk, 10wk, and 16wk old groups. Trabecular separation (Tb.Sp) was greater in the loaded relative to the control tibiae (+12%), and this difference was age-independent (Table 1). Cancellous tissue mineral density (cn.TMD) was 10%, 6%, and 3% greater in the loaded relative to control tibiae for the 6wk, 10wk, and 16wk old groups. In the control limbs, BV/TV and Tb.Th increased from 6wks to 10wks of age and were similar in the 10wk and 16wk old mice (Figure 3, Table 2). Tb.Sp decreased from 6wks to 10wks of age (p=0.003) and was similar between the 10wk and 16wk old mice. In the loaded tibiae, BV/TV was similar in the three age groups, while Tb.Th was greater in the 6wk than the 16wk old mice. In both the loaded and control limbs, cn.TMD was greater in the 10wk and 16wk old mice than in the 6wk old mice.

At the mid-diaphysis, mechanical loading had a strong effect on cortical geometry, and the relative effect of load decreased with age (Figs. 2, 4; Table 1). Cortical cross-sectional area (Ct.Ar) was 43%, 30%, and 17% greater in the loaded relative to control tibiae in the 6wk, 10wk, and 16wk old mice. The maximum moment of inertia (I_{MAX}) increased in the loaded tibiae by 72%, 62%, and 34% compared to control tibiae, while the minimum moment of inertia (I_{MIN}) for the loaded tibiae was greater than the control tibiae by 58%, 30%, and 13%. In the control limbs, Ct.Ar, I_{MAX}, and I_{MIN} increased from 6wks to 10wks of age and were maintained from 10wks to 16wks of age (Figure 4, Table 2). In the loaded limbs, Ct.Ar, I_{MAX}, and I_{MIN} were greatest in the 10wk old mice and similar for the 6 and 16wk old groups.

Cortical TMD (ct.TMD) and bone curvature were generally greater in older mice and not strongly affected by applied load (Table 1). ct.TMD changed slightly, but significantly, with applied load in 6wk and 10wk old mice (+1% and -1%, respectively), but was unaffected by load

in 16wk old mice (Fig. 4, Table 2). The anterior-posterior and medial-lateral radii of curvature (C_{AP} and C_{ML}) increased with age but were unaffected by applied load at any age (Fig. 5; Table 1).

In vivo tibial stiffness changed inversely with applied load in an age-dependent manner. Stiffness was greater in the loaded relative to control tibiae for 6wk old mice (+81%, Fig. 6; Table 1, 2). Tibial stiffness did not differ between loaded and control tibiae in 10wk old mice. In 16wk old mice, tibial stiffness was reduced in the loaded relative to control limbs (-42%). The loaded tibiae of 6wk old mice were stiffer than the loaded tibiae of the two older groups (Figure 6, Table 2). Stiffness did not vary significantly with age in the control limbs. In all mice, tensile (positive) strains were induced on the medial midshaft, during compression loading, due to a combination of AP and ML bending at this site.

Axial and bending stresses induced by a 9N compressive load were less in the loaded than in the control limbs, and this difference decreased with age (Fig. 7; Table 1). In the loaded tibiae, axial stress (σ_{ax}) was 40%, 28%, and 18% lower than in the control tibiae for the 6wk, 10wk, and 16wk old mice. σ_{ax} was similar in the loaded tibiae at all ages and decreased with age in the control limbs (Figure 7, Table 2). Anterior-posterior bending stress ($\sigma_{b,AP}$) in the loaded tibiae was 46%, 27%, and 21% less than in the control tibiae. $\sigma_{b,AP}$ increased with age in the loaded tibiae and was generally similar with age in the control limbs. Medial-lateral bending stress ($\sigma_{b,ML}$) showed a general increase with age and was 33% lower in the loaded relative to the control tibiae across the three age groups (Figure 7; Table 1).

The effects of in vivo loading on tibial length and body mass varied with age. Loaded tibiae were shorter than control tibiae in 6wk old mice (-3%, $p<0.001$), but similar in length for the two older groups ($p>0.75$ for both groups). Body mass increased with age among the groups

and increased over the two week loading period for the 6wk and 10wk old mice, but decreased slightly for the 16wk old mice during the experiment.

Discussion

We examined cancellous and cortical tissue adaptation to two weeks of applied loading in the tibiae of growing and adult female mice and related changes in functional tibial stiffness with loading to cancellous architecture, cortical cross-sectional geometry and longitudinal bone curvature. The anabolic effect of applied load on cancellous and cortical tissue in the tibia decreased with age. In vivo tibial stiffness varied inversely with age in loaded tibiae and remained similar with age in control tibiae. Bone curvature was not affected by applied loading. Changes in tibial stiffness following loading did not directly reflect changes in cross-sectional geometry and bone curvature in 10wk and 16wk old mice, suggesting a load-induced change in bone material properties in older mice. These results clearly demonstrate the importance of measuring post-loading whole bone stiffness to assess bone adaptation to load and demonstrate the limitations of using cross-sectional geometry alone as a surrogate for whole bone structural behaviour.

Two weeks of applied load increased cancellous bone mass in the proximal tibiae of growing and adult mice, and the relative anabolic response decreased with age (Figure 3). Few studies have examined the effect of age on changes in cancellous tissue with applied load. Previously, cancellous tissue in the proximal tibiae of 8wk old C57Bl/6 mice showed an anabolic response to applied load, while bone volume fraction actually decreased with loading in 12 and 20wk old mice (de Souza et al., 2005). Although this previous study found an age-related decrease in the anabolic response to load, similar to our study, the net bone loss reported in the

loaded tibiae at 12wks and 20wks contrasts with the load-induced net gain in bone mass that we measured at 10wks and 16wks of age. These differences may be related to disparities in the load waveform characteristics and/or the total number of load cycles applied between the two studies. Our study applied lower loads (~9N vs. 13N) at a greater frequency (4Hz vs. 2Hz) and for a greater number of cycles per day (1200 vs. 40). The increased cancellous bone mass reported here in the loaded tibiae for the 10wk and 16wk old female C57Bl/6 mice agrees with previous tibial loading studies from our lab for 10wk old male and female C57Bl/6 mice (Fritton et al., 2005; Fritton et al., 2008; Lynch et al., 2010) and with tibial loading experiments using 16wk-19wk old female C57Bl/6 mice (Sugiyama et al., 2008; Sugiyama et al., 2010; Holguin et al., 2013). The decreased anabolic cancellous response to applied load with age from 6wks to 16wks of age found here is consistent with our previous work showing a decrease in the cancellous response from 10wks to 26wks of age (Lynch et al., 2011).

Similar to our cancellous results, applied load increased cortical bone mass at all three ages, and the relative adaptive response decreased with age. These results agree with previous studies reporting decreased cortical adaptation with age to a given applied strain magnitude (Rubin et al., 1992; Turner et al., 1995; Srinivasan et al., 2003; Lynch et al., 2011). In cancellous tissue, all three age groups achieved similar values for BV/TV and Tb.Th in the loaded limbs. In cortical bone, the relative anabolic response was greatest in 6wk old mice, but the greatest cortical geometries were achieved in the loaded tibiae of 10wk old mice. Although the absolute magnitude of the cortical area increase in the tibial midshaft was less in 10wk than in 6wk old mice, the larger cortical area in the 10wk old mice at the start of the experiment (Main et al., 2010) led to a larger cortical cross-section in the 10wk old mice following loading. Further studies are needed to verify the long-term effects of tissue adaptation on cortical and

cancellous bone mass in the different age groups examined in this study. The positive effects of exercise during growth on adult bone mass, even following cessation of activity, has been shown in human athletes and rodent loading models (Warden et al., 2007; Erlandson et al., 2012).

Two weeks of applied load altered tibial stiffness in an age-dependent manner. In the 6wk old mice, stiffness increased in the loaded relative to the control tibiae, while stiffness was similar and decreased in the loaded relative to control tibiae in 10wk and 16wk old mice, respectively. While tibial stiffness was independent of age in the control limbs, the loaded tibiae of 6wk old mice were stiffer than either the loaded or control tibiae of the 10wk or 16wk old mice. Increased stiffness in the loaded tibiae of 6wk old mice is consistent with this group having the greatest load-induced increase in cortical geometry and largest decrease in load-induced stress. The increased cortical geometry and reduced stresses with loading in 10wk old mice may have been insufficient to produce a measurable increase in tibial stiffness following loading. Given the load-induced increase in cortical geometry in 16wk old mice, reduced stiffness in the loaded tibiae for this group must reflect decreased tissue material properties at the level of gauge attachment.

The midshaft cortical tissue was examined for microcracks in the three age groups, using basic fuchsin, to verify that decreased stiffness in the loaded tibiae of 16wk old mice was not caused by load-induced damage. Microcracks were not present in the diaphyseal cortices of the loaded tibiae at any age (pers. comm., Dr. M. Schaffler). Thus, the decreased stiffness in the loaded tibiae at 16wks of age must reflect altered material properties in the bone tissue itself at the site of the stiffness measures. Target strain levels in the present study were chosen based upon in vivo studies showing that 1200με corresponds to moderate levels of activity in many vertebrates (Rubin and Lanyon 1982, Biewener 1993), including mice (Lee et al., 2002;

Sugiyama et al., 2012). Previously, even greater compressive loads than those used in this study (13N), that induced -1500με on the medial tibia, did not cause microdamage in 12wk old mice (de Souza et al. 2005). Although in vivo loading can have clear anabolic effects on skeletal geometry, the influence of long-term loading protocols on mineral and collagen physiochemical properties have not been well characterized. Using Raman microspectroscopy, two related studies found increased mineral:matrix ratios in growing and adult male mice following 21 days of treadmill exercise (Kohn et al., 2009; Wallace et al., 2010). Collagen cross-linking also increased in C3H mice, but not B6/129 mice (Wallace et al., 2010). The greater mechanical stimulus provided by tibial loading in our study, relative to these exercise studies, may have produced age-related changes in tissue properties, such as the degree of mineralization or collagen cross-linking, that were detrimental to tissue material properties in the older mice. Changes in these tissue properties might not be detectable by microcomputed tomography (microCT).

Histomorphometric and microCT analyses are used in many applied loading studies to measure adaptive increases in bone mass (Rubin et al., 1992; Robling et al., 2001; Gross et al, 2002; Fritton et al, 2005; de Souza et al., 2005) and/or estimate changes in load-induced bone strains (Turner et al., 1995; Akhter et al., 1998; Robling and Turner et al., 2002), often without accompanying structural or material tests. However, as shown in this study, increased mid-diaphyseal cross-sectional geometry does not necessarily increase whole bone stiffness during axial compression loading in the tibia, illustrating the importance of structural or material tests to more fully assess bone adaptation to load. Geometric analyses alone do not provide information regarding changes in tissue composition or material properties (van der Meulen et al., 2001). A previous comparison of ulnar strains measured in baseline rats and following applied loading

found decreased ex vivo bone strains and increased bone strength in adult rat ulnae post-loading (Robling et al. 2002), in contrast to the decreased tibial stiffness with loading found here for adult mice tibiae. However, greater absolute strains were induced during loading (-3300με vs. 1200με) for a longer period of time (16wks vs. 2wks) than in the present study, resulting in I_{MIN} increases of 70-100% in the loaded relative to the control limbs compared to a 13% increase in I_{MIN} here. The conflicting stiffness results, despite load-induced increases in bone geometry in both studies, highlight the value of measuring whole bone mechanical function following loading through whole bone stiffness tests, when the goal is to investigate physical methods for increasing bone mass and strength or stiffness.

The "whole bone" stiffness measures made in this study are from in vivo mechanical tests incorporating the length of the entire bone, not the diaphysis of excised bones. In this study, stiffness was measured at a single site on the medial surface of the tibia near the midshaft. Measuring stiffness at different sites on the tibia could produce different post-loading results given regional differences in the anabolic response to load and the complex geometry of the tibia. Differential changes in post-loading stiffness may even occur at different sites on the midshaft where the periosteal anabolic response to applied loads is likely non-uniform. More comprehensive measures of stiffness, such as finite element modeling approaches, could potentially address these limitations.

Recently, load-induced strains in experimentally loaded and contralateral mouse tibiae were compared using a digital image correlation method (Sztefek et al., 2010). Two weeks of tibial loading in 8wk old male mice subjected to 12N compressive loads did not significantly decrease average peak strains on the medial surface of the tibia, similar to our results in 10wk old female mice. However, the load-induced changes in bone geometry or curvature were not

reported for this study, so the structural or material causes for these results cannot be evaluated. Given the decreased stiffness with load reported here in 16wk old mice, despite increased cortical geometry, the lack of tissue material property analyses is a limitation of our study. At the tissue level, nanoindentation, FTIR, or Raman analyses could identify the time course of material property and compositional changes in newly formed and existing bone tissue to further understand changes in bone structural stiffness or strength with age and load (Busa et al. 2005, Gourion-Arsiquaud et al. 2009, Kohn et al. 2009, Donnelly et al. 2009).

Bone curvature is a critical determinant of bone stress and, ultimately, stiffness during skeletal loading. Increased curvature with age is responsible for maintenance of functional tibial stiffness despite age-related increases in bone geometry in the control limbs, similar to previous findings for mice between 6 and 16wks of age (Main et al., 2010). Two weeks of applied load did not significantly alter tibial curvature and thus, did not contribute to the changes in functional stiffness measured for the loaded tibiae. The maintenance of bone curvature following loading in our study contrasts with the decreased curvature following applied loading in rat ulnae (Mosley et al. 1997). The differential effects of applied load on bone curvature in these two studies may be related to differences in the biological response of the rat ulna and mouse tibia to load, the magnitudes of the induced strains (-2000με vs. 1200με), or the methods for measuring curvature. Cortical geometry *and* whole bone morphology are important determinants of functional bone stiffness and the loading environment engendered in the tissue (Lanyon 1987) and should be considered more widely in functional adaptation and comparative skeletal biomechanics studies.

In summary, in vivo tibial loading is anabolic in both cancellous and cortical compartments in the mouse tibia and increases functional in vivo stiffness in 6wk old mice. Two

weeks of applied loading to induce 1200με tissue deformations at the medial tibial mid-diaphysis increased cancellous bone mass and cortical geometry and decreased tissue stresses more in growing than adult female mice. Post-adaptation in vivo stiffness measurements showed that increased cortical geometry with loading increased tibial stiffness in young mice, but decreased stiffness in adult mice. As load-induced damage was not present in the loaded tibiae at any age, the decrease in stiffness with loading in 16wk old mice may be due to alterations in tissue material properties that will be explored further in future studies. Measures of whole bone stiffness and morphology in conjunction with histological and material property assessments of bone's response to load are important in understanding the transmission of load through the skeleton and the functional adaptation of bones to mechanical loads.

Materials and Methods

Experimental in vivo tibial loading

Dynamic compressive loads were applied to the left tibiae of 6wk (N=16), 10wk (N=6), and 16wk old (N=18) female C57Bl/6 mice (*Mus musculus*, Linnaeus; Jackson Labs, Bar Harbor, ME). At the start of the experiment, the average body masses of the separate 6wk, 10wk, and 16wk old experimental groups were 15.7g, 18.6g, and 21.6g, respectively. At 6wks of age, mice are rapidly growing and post-pubescent (Sheng et al. 1999, Richman et al. 2001, Somerville et al. 2004). Female C57Bl/6 mice are considered mature adults by 16wks of age (Flurkey et al., 2007), active growth has decreased, and peak bone mass is achieved (Beamer et al. 1996, Sheng et al. 1999, Somerville et al. 2004). Ten weeks is an intermediate age that was used in our previous loading experiments (Fritton et al., 2005; Fritton et al., 2008; Lynch et al., 2010). The 10wk old mice were included in this study primarily to measure changes in tibial stiffness

following loading that were not examined in our previous studies focusing on the morphologic response of the tibia to applied load (Lynch et al., 2010) or examining age-related changes in the morphologic determinants of tibial stiffness (Main et al., 2010). Previous work from our group has shown that age-related differences in tibial stiffness can be determined using N=5 mice per experimental group (Lynch et al., 2010; Lynch et al., 2011). Despite the smaller sample size for the 10wk old group, their morphometric data are also included for comparison to the 6wk and 16wk old mice.

Compressive loads were applied to the left tibia of each mouse for two weeks using a custom loading device (Fritton et al., 2005; Main et al., 2010). Briefly, the loading device holds the knee in a small brass cup while applying dynamic compressive loads at the foot by displacement of an electromagnetic linear actuator (Fig. 1), controlled by force feedback using custom-written software (Labview, v.8.5, National Instruments, Austin, TX). The force transmitted through the tibia to the knee is measured using a load cell placed in line with the knee cup (ELFS-T3E-20L, Measurement Specialties, Inc., Hampton, VA). Using an osteogenic protocol validated in previous studies from our group (Lynch et al., 2010; Lynch et al., 2011), triangle waveform loads were applied 5 days/wk (Days 1-5, 8-12) for 1200 cycles/day at 4Hz while the animals were anesthetized (2% isoflurane, 1.0 L/min O_2). The loading waveform was characterized by 0.15sec of loading/unloading with a 0.10sec 'rest phase' between load cycles (Fig. 1) (Lynch et al., 2010). Based upon previously established age-related differences in tibial stiffness in these age groups (Main et al., 2010), peak applied loads were adjusted for each age group at the start of the experiments to induce 1200με on the medial surface of the tibial midshaft. This strain level is characteristic of moderate activity levels in rodents and a variety of vertebrates (Rubin and Lanyon, 1982; Biewener, 1993; Mosley et al., 1997; Rabkin et al., 2001).

Peak loads of -9.1N, -9.1N, and -8.8N and 'rest phase' loads of -1.5N, -1.7N, and -1.7N were applied to the tibiae of the 6wk, 10wk, and 16wk old mice, respectively. The timing of the loading cycle was maintained across the three age groups. The right tibia served as a non-loaded control. Mice were housed 4-5 per cage and maintained on a 12:12 light-dark cycle. Mice were allowed normal cage activity and ad libitum access to commercial rodent diet and water between loading sessions.

In vivo tibial stiffness was measured at the end of the two weeks of loading (Day 15) for the loaded and control tibiae in a randomly chosen subset of mice from the 6wk and 16wk age groups and the entire 10wk group (N=6/group). While mice were anesthetized, tibial stiffness was measured using a single element strain gauge attached to the midshaft of the medial surface of the tibia following methods detailed previously (Main et al., 2010). Stiffness was measured over a range of compressive loads (Main et al., 2010) and was calculated as the change in load over the change in strain ($\Delta\mu\varepsilon$, $\varepsilon \times 10^{-6}$) during the loading portion of the waveform and averaged across four consecutive load cycles. Stiffness data were excluded if the strain gauge was placed greater than 6% of the tibia's length from the midshaft, leaving N=3, 3, and 4 mice for the 6wk, 10wk, and 16wk old groups. Both strain gauge location and tibial length were determined by microcomputed tomography (microCT, see below). These sample sizes are similar to or greater than those used to establish load-strain stiffness relationships in other in vivo loading studies (de Souza et al., 2005; Fritton et al., 2005; Gross et al., 2002; Hsieh et al., 2001; Lee et al., 2002; Robling and Turner, 2002; Warden et al., 2007). On Day 15, the mice weighed 16.3g, 19.1g, and 21.0g on average for the three age groups, respectively. Mice were euthanized by carbon dioxide inhalation. The tibiae were dissected free of soft tissue, fixed in 10% neutral buffered formalin

386 for 24hr, then stored in 70% ethanol at room temperature. All experimental procedures were
387 approved by the Cornell University IACUC.
388
389 *Morphometric and stress analyses*
390 Post-loading morphometric analyses were conducted for the loaded and control tibiae in the 6wk
391 (N=10), 10wk (N=6), and 16wk (N=12) old mice by microCT. In the 10wk old mice, the solder
392 leads were removed from the strain gauge-instrumented tibiae prior to scanning. Two pairs of
393 loaded and control tibiae were scanned together in phosphate-buffered saline (μCT 35, Scanco
394 Medical, Brüttisellen, Switzerland; 55kVp, 145μA, 600ms integration time, no frame averaging).
395 A 0.5mm aluminum filter reduced the effects of beam hardening (Meganck et al., 2009). Scans
396 of the proximal tibial metaphyses and cortical mid-diaphyses were made at a 15μm isotropic
397 voxel resolution. Whole tibiae from the experimental loading group and the strain-gauged tibiae
398 from the mice used for tibial stiffness measures were scanned with a voxel resolution of 20μm
399 using similar settings. Following scanning, whole bone and diaphyseal cortical segments were
400 aligned using anatomical landmarks. Specifically, the point at which the fibular marrow canal
401 bifurcates from the tibial marrow canal was digitally aligned with the tibiofibular junction along
402 the z-axis of the scan using a custom script in the manufacturer's software (Main et al., 2010). A
403 hydroxyapatite (HA) calibration phantom provided by the manufacturer was used to convert the
404 linear attenuation for each voxel to g HA/cm^3 for all scans.
405 Cortical and cancellous volumes of interest (VOIs) were analyzed. The purely cancellous
406 VOIs in the proximal tibial metaphysis began distal to the growth plate, excluding the primary
407 spongiosa and cortical shell, and extended 10% of the total tibial length. Age-specific thresholds
408 were used to segment mineralized tissue from water and soft tissue (0.25, 0.26, and 0.27 g

HA/cm^3 for the 6wk, 10wk, and 16wk old groups) (Halloran et al., 2002; Miller et al., 2007). Cancellous measures included bone volume fraction (BV/TV), cancellous tissue mineral density (cn.TMD, mg HA/cm^3), and trabecular thickness and separation (Tb.Th and Tb.Sp, μm). Cortical VOIs were centered at the midshaft and extended proximal-distally a total of 2.5% of the bone's length. Age-specific thresholds were set at one third of the bone peak of the x-ray attenuation histogram, resulting in 0.28, 0.30, and 0.31 g HA/cm^3 for the 6wk, 10wk, and 16wk old groups, which are similar to the threshold values used previously for these age groups (Main et al., 2010). Cortical measures included cortical area (Ct.Ar, mm^2), principal moments of inertia (I_{MAX}, I_{MIN}, mm^4), and cortical tissue mineral density (ct.TMD, g HA/cm^3). The relative lengths of the cancellous and cortical VOIs are consistent with the VOIs used by our group previously (Fritton et al., 2005; Lynch et al., 2010; Main et al., 2010; Lynch et al., 2011). Different threshold values for cortical and cancellous volumes have been used previously (Halloran et al., 2002; Lynch et al., 2011).

The anterior-posterior and medial-lateral radii of curvature (C_{AP} and C_{ML}, mm) were measured on whole bone scans of the instrumented tibiae using previously published methods (Main et al., 2010). Briefly, C_{AP} and C_{ML} were measured as the perpendicular distances between reference lines passing through the midpoints of the proximal and distal ends of each tibia and the AP and ML midpoints of the bone at mid-gauge level. Positive values for C_{AP} and C_{ML} represent anterior and medial convexities, respectively. Bone length and AP and ML bone diameters at the level of the strain gauge were also measured using the 20μm resolution scans.

Axial and bending stresses induced by a 9N compressive axial load were calculated for the instrumented tibiae at the level of the strain gauge to provide insight into how morphological changes with age and loading influence the measured tibial stiffness (N=3, 3, 4 for the 6wk,

10wk, and 16wk old mice). Although the three age groups received slightly different peak loads during the in vivo loading experiments, a single average load was used for the stress calculations to facilitate comparison of the effects of bone morphology on load-induced stresses. The axial (σ_{ax}, MPa) and AP and ML bending stresses ($\sigma_{b,AP}$, $\sigma_{b,ML}$, MPa) induced by the compressive load were calculated using beam theory (Biewener, 1983a; Main et al., 2010). Due to the typically convex anterior and medial curvatures of the tibiae at the gauge site, σ_b is positive (tensile) on the anterior and medial bone surfaces. This stress and strain distribution for the tibial diaphysis is confirmed by previous combined finite element and strain gauge analyses of the tibia under compressive load (Stadelmann et al., 2009; Moustafa et al., 2012; Patel et al., 2013; Willie et al., 2013). The tibia experiences a combination of axial compression and medial-lateral and anterior-posterior bending that places the medial and anterior regions of the bone in tension and the posterior and lateral regions of the bone in compression.

Statistical analyses

The effects of age and loading and the interaction of these factors on tibial stiffness and cancellous and cortical morphology were examined using a linear mixed model with repeated measures. The between-subject factor was age (6wks, 10wks, or 16wks old) and the within-subject factor was limb (loaded or control). When the interaction term was significant, specific differences between the limbs and/or age groups were tested by pair-wise comparisons with a Bonferroni correction for multiple comparisons (PASW Statistics, v.18, SPSS). Percent differences between the loaded and control tibiae were calculated as: [(loaded-control)/control x 100]. Data are presented as mean + s.d. Statistical significance is indicated at $p < 0.05$. Only significant results are reported unless otherwise stated.

Acknowledgments

We thank Thomas Schmicker, Daniel Walsh, Casey Boyle, Sarah Yagerman, and Frank Ko for their help in conducting the experiments and analyses and Dr. Mitch Schaffler for conducting the cortical microcrack analyses.

Funding

This work was supported by the National Institutes of Health [R01-AG028664 and P30-AR46121 to MCHvdM, F32-AR054676 to RPM] and the National Science Foundation [NSF GRF to MEL]. The content in this paper is the responsibility of the authors and does not necessarily represent the official views of the individual granting agencies within the National Institutes of Health.

List of Symbols and Abbreviations

BV/TV: bone volume fraction
C_{AP}: anterior-posterior bone curvature
C_{ML}: medial-lateral bone curvature
cnTMD: cancellous tissue mineral density
Ct.Ar: cortical area
ctTMD: cortical tissue mineral density
HA: hydroxyapatite
I_{MAX}: maximum moment of inertia
I_{MIN}: minimum moment of inertia
Tb.Th: trabecular thickness
Tb.Sp: trabecular separation
VOI: volume of interest
με: microstrain (strain x 10^{-6})
σ_{ax}: axial stress
$\sigma_{b,AP}$: anterior-posterior bending stress
$\sigma_{b,ML}$: medial-lateral bending stress

References

Akhter M.P., Cullen D.M., Pedersen E.A., Kimmel D.B. and Recker R.R. (1998). Bone response to *in vivo* mechanical loading in two breeds of mice. *Calcif. Tissue Int.* **63**, 442-449.

Bass S.L., Saxon L., Daly R.M., Turner C.H., Robling A.G., Seeman E. and Stuckey S. (2002). The effect of mechanical loading on the size and shape of bone in pre-, peri-, and postpubertal girls: a study in tennis players. *J. Bone Miner. Res.* **17**, 2274-2280.

Beamer W.G., Donahue L.R., Rosen C.J. and Baylink D.J. (1996). Genetic variability in adult bone density among inbred strains of mice. *Bone* **18**, 397-403.

Biewener A.A. (1983a). Locomotory stresses in the limb bones of two small mammals: the ground squirrel and chipmunk. *J. Exp. Biol.* **103**, 131-154.

Biewener, A.A. (1983b). Allometry of quadrupedal locomotion: the scaling of duty factor, bone curvature and limb orientation to body size. *J. Exp. Biol.* **105**, 147-171.

Biewener A.A. (1993). Safety factors in bone strength. *Calcif. Tissue Int.* **53(Suppl. 1)**, S68-S74.

Biewener A.A. and Bertram J.E.A. (1994). Structural response of growing bone to exercise and disuse. *J. Appl. Physiol.* **76**, 946-955.

Busa B., Miller L.M., Rubin C.T., Qin Y-X and Judex S. (2005). Rapid establishment of chemical and mechanical properties during lamellar bone formation. *Calcif. Tissue Int.* **77**, 386-394.

Carter D.R. (1982). The relationship between in vivo strains and cortical bone remodeling. *Crit. Rev. Biomed. Eng.* **8**, 1-27.

de Souza R.L., Matsuura M., Eckstein F., Rawlinson S.C.F., Lanyon L.E. and Pitsillides A.A. (2005). Non-invasive axial loading of mouse tibiae increases cortical bone formation and modifies trabecular organization: a new model to study cortical and cancellous compartments in a single loaded element. *Bone* **37**, 810-818.

Dodge, T., Wanis, M., Ayoub, R., Zhao, L., Watts, N.B., Bhattacharya, A., Akkus, O., Robling, A., and Yokota, H. (2012). Mechanical loading, damping, and load-driven bone formation in mouse tibiae. *Bone* **51**, 810-818.

Donnelly E., Boskey A.L., Baker S.P. and van der Meulen M.C.H. (2009). Effects of tissue age on bone material composition and nanomechanical properties in the rat cortex. *J. Biomed. Mater. Res. A* **92A**, 1048-1056.

Erlandson, M. C., Kontulainen, S.A., Chilibeck, P.D., Arnold, C.M., Faulkner, R.A. and Baxter-Jones, A.D.G. (2012). Higher premenarcheal bone mass in elite gymnasts is maintained into young adulthood after long-term retirement from sport: A 14-year follow-up. *J. Bone Miner. Res.* **27,** 104-110.

Flurkey, K., Currer, J.M. and Harrison, D.E. (2007). Mouse models in aging research. In The Mouse in Biomedical Research, J.G. Fox, M.T. Davisson, F.W. Quimby, S.W. Barthold, C.E. Newcomer, and A.L. Smith, eds. (Amsterdam: Academic Press), pp. 637-672.

Fritton J.C., Myers E.R., Wright T.M. and van der Meulen M.C.H. (2005). Loading induces site-specific increases in mineral content assessed by microcomputed tomography of the mouse tibia. *Bone* **36**, 1030-1038.

Fritton J.C., Myers E.R., Wright T.M. and van der Meulen M.C.H. (2008). Bone mass is preserved and cancellous architecture altered due to cyclic loading of the mouse tibia after orchidectomy. *J. Bone Miner. Res.* **23**, 663-671.

Frost H.M. (1983). A determinant of bone architecture: the minimum effective strain. *Clin. Orthop. Relat. R.* **175**, 286-292.

Gourion-Arsiquaud S., Burket J.C., Havill L.M., DiCarlo E., Doty S.B., Mendelsohn R., van der Meulen M.C.H. and Boskey A.L. (2009). Spatial variation in osteonal bone properties relative to tissue and animal age. *J. Bone Miner. Res.* **24**, 1271-1281.

Gross T.S., Srinivasan S., Liu C.C., Clemens T.L. and Bain S.D. (2002). Noninvasive loading of the murine tibia: an in vivo model for the study of mechanotransduction. *J. Bone Miner. Res.* **17**, 493-501.

Haapasalo H., Kannus P., Sievanen H., Pasanen M., Uusi-Rasi K., Heinonen A., Oja P. and Vuori I. (1998). Effect of long-term unilateral activity on bone mineral density of female junior tennis players. *J. Bone Miner. Res.* **13**, 310-319.

Halloran, B.P., Ferguson, V.L., Simske, S.J., Burghardt, A., Venton, L.L., and Majumdar, S. (2002). Changes in bone structure and mass with advancing age in the male C57Bl/6 mouse. *J. Bone Miner. Res.* **17,** 1044-1050.

Holguin, N., Brodt, M.D., Sanchez, M.E., Kotiya, A.A., and Silva, M.J. (2013). Adaptation of tibial structure and strength to axial compression depends on loading history in both C57Bl/6 and BALB/c mice. *Calcif. Tissue Int.* **93**, 211-221.

Hsieh, Y.-F., Robling, A.G., Ambrosius, W.T., Burr, D.B., and Turner, C.H. (2001). Mechancal loading of diaphyseal bone in vivo: the strain threshold for an osteogenic response varies with location. *J. Bone Miner. Res.* **16**, 2291-2297.

Jones H.H., Priest, J.D., Hayes, W.C., Tichenor C.C., Nagel, D.A. (1977). Humeral hypertrophy in response to exercise. *J. Bone Jt. Surg. Am.* **59**, 204-208.

Kannus P., Haapasalo H., Sankelo M., Sievanen H., Pasanen M., Heinonen A., Oja P. and Vuori I. (1995). Effect of starting age of physical activity on bone mass in the dominant arm of tennis and squash players. *Ann. Intern. Med.* **123**, 27-31.

Kohn D.H., Sahar N.D., Wallace J.M., Golcuk K. and Morris M.D. (2009). Exercise alters mineral and matrix composition in the absence of adding new bone. *Cells Tissues Organs* **189**, 33-37.

Lang, T., Leblanc, A., Evans, H., Lu, Y., Genant, H. and Yu, A. (2004). Cortical and trabecular bone mineral loss from the spine and hip in long-duration spaceflight. *J. Bone Miner. Res.* **19**, 1006-1012.

Lanyon L.E. (1980). The influence of function on the development of bone curvature. An experimental study on the rat tibia. *J. Zool., Lond.* **192**, 457-466.

Lanyon L.E., Goodship A.E., Pye C.J. and MacFie J.H. (1982). Mechanically adaptive bone remodeling. *J. Biomech.* **15**, 141-154.

Lanyon L.E. (1987). Functional strain in bone tissue as an objective, and controlling stimulus for adaptive bone remodelling. *J. Biomech.* **20**, 1083-1093.

Lee K.C.L, Maxwell A. and Lanyon L.E. (2002). Validation of a technique for studying functional adaptation of the mouse ulna in response to mechanical loading. *Bone* **31**, 1-9.

Lynch, M.E., Main, R.P., Xu, Q., Walsh, D.J., Schaffler, M.B., Wright, T.M. and van der Meulen, M.C.H. (2010). Cancellous bone adaptation to tibial compression is not sex dependent in growing mice. *J. Appl. Physiol.* **109**, 685-691.

Lynch, M.E., Main, R.P., Xu, Q., Schmicker, T.L., Schaffler, M.B., Wright, T.M. and van der Meulen, M.C.H. (2011). Tibial compression is anabolic in the adult mouse skeleton despite reduced responsiveness with aging. *Bone* **49**, 439-446.

Main R.P., Lynch M.E. and van der Meulen M.C.H. (2010). In vivo tibial stiffness is maintained by whole bone morphology and cross-sectional geometry in growing female mice. *J. Biomech.* **43**, 2689-2694.

Meganck, J.A., Kozloff, K.M., Thornton, M.M., Broski, S.M., and Goldstein, S.A. (2009). Beam hardening artifacts in micro-computed tomography scanning can be reduced by X-ray beam filtration and the resulting images can be used to accurately measure BMD. *Bone* **45**, 1104-1116.

Melton L.J., Gabriel S.E., Crowson C.S., Tosteson A.N.A., Johnell O. and Kanis J.A. (2003). Cost-equivalence of different osteoporotic fractures. *Osteoporos. Int.* **14**, 383-388.

Miller, L.M., Little, W., Schirmer, A., Sheik, F., Busa, B., and Judex, S. (2007). Accretion of bone quantity and quality in the developing mouse skeleton. *J. Bone Miner. Res.* **22**, 1037-1045.

Mosley J.R., March B.M., Lynch J. and Lanyon L.E. (1997). Strain magnitude related changes in whole bone architecture in growing rats. *Bone* **20**, 191-198.

Patel, T.K., Brodt, M.D., and Silva, M.J. (2013). Experimental and finite element analysis of strains induced by axial tibial compression in young-adult and old female C57Bl/6 mice. *J. Biomech.* doi: 10.1016/j.jbiomech.2013.10.052. [Epub ahead of print]

Rabkin B.A., Szivek J.A., Schonfeld J.E. and Halloran B.P. (2001). Long-term measurement of bone strain *in vivo*: the rat tibia. *J. Biomed. Mater. Res.* **58**, 277-281.

Richman C., Kutilek S., Miyakoshi N., Srivastava A.K., Beamer W.G., Donahue L.R., Rosen C.J., Wergedal J.E., Baylink D.J. and Mohan S. (2001). Postnatal and pubertal skeletal changes contribute predominantly to the differences in peak bone density between C3H/HeJ and C57Bl/6J mice. *J. Bone Miner. Res.* **16**, 386-397.

Robling A.G., Duijvelaar K.M., Geevers J.V., Ohashi N. and Turner C.H. (2001). Modulation of appositional and longitudinal bone growth in the rat ulna by applied static and dynamic force. *Bone* **29**, 105-113.

Robling, A.G., and Turner, C.H. (2002). Mechanotransduction in bone: genetic effects on mechanosensitivity in mice. *Bone* **31**, 562-569.

Robling A.G., Hinant F.M., Burr D.B. and Turner C.H. (2002). Improved bone structure and strength after long-term mechanical loading is greatest if loading is separated into short bouts. *J. Bone Miner. Res.* **17**, 1545-1554.

Rubin C.T. and Lanyon L.E. (1982). Limb mechanics as a function of speed and gait: a study of functional strains in the radius and tibia of horse and dog. *J. Exp. Biol.* **101**, 187-211.

Rubin C.T., Bain S.D. and McLeod K.J. (1992). Suppression of the osteogenic response in the aging skeleton. *Calcif. Tissue Int.* **50**, 306-313.

Ruff C.B., Walker A. and Trinkaus E. (1994). Postcranial robusticity in *Homo*. III: Ontogeny. *Am. J. Phys. Anthropol.* **93**, 35-54.

Sheng M.H-C., Baylink D.J., Beamer W.G., Donahue L.R., Rosen C.J., Lau K-H.W. and Wergedal J.E. (1999). Histomorphometric studies show that bone formation and bone mineral apposition rates are greater in C3H/HeJ (high-density) than C57Bl/6J (low-density) mice during growth. *Bone* **25**, 421-429.

Sievanen, H. (2010). Immobilization and bone structure in humans. *Arch. Biochem. Biophys.* **503**, 146-152.

Somerville J.M., Aspden R.M., Armour K.E., Armour K.J. and Reid D.M. (2004). Growth of C57Bl/6 mice and the material and mechanical properties of cortical bone from the tibia. *Calcif. Tissue Int.* **74**, 469-475.

Srinivasan S., Agans S.C., King K.A., Moy N.Y., Poliachik S.L. and Gross T.S. (2003). Enabling bone formation in the aged skeleton via rest-inserted mechanical loading. *Bone* **33**, 946-955.

Stadelmann, V.A., Hocke, J., Verhelle, J., Forster, V., Merlini, F., Terrier, A., and Pioletti, D.P. (2009). 3D strain map of axially loaded mouse tibia: a numerical analysis validated by experimental measurements. *Comput Method Biomec* **12,** 95-100.

S**ugiyama T., Saxon L.K., Zaman G., Moustafa A., Sunters A., Price J.S. and Lanyon L.E.** (2008). Mechanical loading enhances the anabolic effects of intermittent parathyroid hormone (1-34) on trabecular and cortical bone in mice. *Bone* **43**, 238-248.

Sugiyama T., Price J.S. and Lanyon L.E. (2010). Functional adaptation to mechanical loading in both cortical and cancellous bone is controlled locally and is confined to the loaded bones. *Bone* **46**, 314-321.

Sugiyama T., Meakin, L.B., Browne, W.J., Galea, G.L., Price J.S. and Lanyon L.E. (2012). Bones' adaptive response to mechanical loading is essentially linear between the low strains associated with disuse and the high strains associated with the lamellar/woven bone transition. *J. Bone Miner. Res.* **27**, 1784-1793.

Sztefek P., Vanleene M., Olsson R., Collinson R., Pitsillides, A.A. and Shefelbine, S. (2010). Using digital image correlation to determine bone surface strains during loading and after adaptation of the mouse tibia. *J. Biomech.* **43**, 599-605.

Turner C.H., Takano Y. and Owan I. (1995). Aging changes mechanical loading thresholds for bone formation in rats. *J. Bone Miner. Res.* **10**, 1544-1549.

van der Meulen M.C.H., Jepsen K.J. and Mikic B. (2001). Understanding bone strength: size isn't everything. *Bone* **29**, 101-104.

Wallace, J.M., Goluck, K., Morris, M.D., and Kohn, D.H. (2010). Inbred strain-specific effects of exercise in wild type and biglycan deficient mice. *Ann. Biomed. Eng.* **38**, 1607-1617.

Warden, S.J., Hurst, J.A., Sanders, M.S., Turner, C.H., Burr, D.B. and Li, J. (2005). Bone adaptation to a mechanical loading program significantly increases skeletal fatigue resistance. *J. Bone Miner. Res.* **20**, 809-816.

Warden, S. J., Fuchs, R.K., Castillo, A.B., Nelson, I.R. and Turner, C.H. (2007). Exercise when young provides lifelong benefits to bone structure and strength. *J. Bone Miner. Res.* **22,** 251-259.

Figure Legends

Figure 1. Device used to load the hindlimbs of 6wk, 10wk, and 16wk old female C57Bl/6 mice. Compressive loads were applied at the foot using an electromagnetic actuator and transmitted loads were measured with a load cell at the knee. Load was transmitted to the tibia (in white) through the calcaneus and the femur (in black). The triangle waveform (0.075s load, 0.075s unload, 0.100s "rest phase") was applied in series 1200 times per load session (~5 minutes of cyclic loading per day), 5 days/week for 2 weeks.

Figure 2. (A) Frontal sections through the proximal tibial metaphyses (0.26mm thick) and (B) transverse sections through the tibial mid-diaphyses (0.43mm thick) from representative microCT reconstructions of the loaded and control tibiae for the 6wk, 10wk, and 16wk old groups examined.

Figure 3. Changes in cancellous tissue of the proximal tibial metaphyses with applied load for 6wk, 10wk, and 16wk old mice. (A) Bone volume fraction, BV/TV, (B) trabecular thickness, Tb.Th, (C) trabecular separation, Tb.Sp, and (D) cancellous tissue mineral density, cn.TMD. Values shown are mean (+ 1 s.d.). Data for the control and loaded tibiae are shown in black and white, respectively. The letters above a given bar (or bracketed pair of bars) indicate a statistically significant difference ($p<0.05$) between groups with different letters and a lack of difference for groups with similar letters, by linear mixed model with repeated measures, followed by pair-wise comparisons with Bonferroni correction. Letters and brackets above the pairs of data bars in (C) indicate age-related main effect differences. Asterisks (*) next to the age

group labels in (C) indicate a main effect difference between the loaded and control limbs across the three age groups corresponding to a general increase in Tb.Sp in the loaded tibiae.

Figure 4. Changes in the tibial mid-diaphysis with applied load for the 6wk, 10wk, and 16wk old mice. (A) Cortical area, Ct.Ar, (B) maximum moment of inertia, I_{MAX}, (C) minimum moment of inertia, I_{MIN}, and (D) cortical tissue mineral density, ct.TMD. Values shown are mean (+ 1 s.d.) Data for the control and loaded tibiae are shown in black and white, respectively. Different letters between bars indicate significant differences in the means by linear mixed model with repeated measures, followed by pair-wise comparisons with Bonferroni correction ($p < 0.05$). See Figure 3 legend for further details regarding the lettering scheme.

Figure 5. Longitudinal tibial curvature in the loaded and unloaded limbs of the 6wk, 10wk, and 16wk old mice. (A) Anterior-posterior, C_{AP} and (B) medial-lateral curvature, C_{ML} are shown as mean (+ 1 s.d.). Data for the control and loaded tibiae are shown in black and white, respectively. The different letters above each pair of bars represent significant main effect differences with age at $p < 0.05$ by linear mixed model with repeated measures. See Figure 3 legend for further details regarding the lettering scheme. Applied load had no effect on bone curvature for any age group.

Figure 6. In vivo tibial stiffness measurements for the loaded and control tibiae for the 6wk, 10wk, and 16wk old mice. Values shown are means (– 1 s.d.). Data for the control and loaded tibiae are shown in black and white, respectively. Different letters between bars indicate significant differences in the means by linear mixed model with repeated measures, followed by

pair-wise comparisons with Bonferroni correction ($p < 0.05$). See Figure 3 legend for further details regarding the lettering scheme.

Figure 7. Stress calculations for the loaded and control tibiae under a 9N axial compressive load for the 6wk, 10wk, and 16wk old mice. (A) axial stress, σ_{ax}, (B) anterior-posterior bending stress, $\sigma_{b,AP}$, and (C) medial-lateral bending stress, $\sigma_{b,ML}$. Values shown are means (± 1 s.d.). Data for the control and loaded tibiae are shown in black and white, respectively. Different letters between bars or pairs of bars indicate significant differences in the means by linear mixed model with repeated measures, followed by pair-wise comparisons with Bonferroni correction ($p < 0.05$). See Figure 3 legend for further details regarding the lettering scheme. Letters and brackets above the pairs of data bars in (C) indicate main effect differences with age. Asterisks (*) next to the age group labels in (C) indicate a main effect difference between the loaded and control limbs across the three age groups corresponding to a general decrease in $\sigma_{b,ML}$ in the loaded tibiae.

FIGURE 1

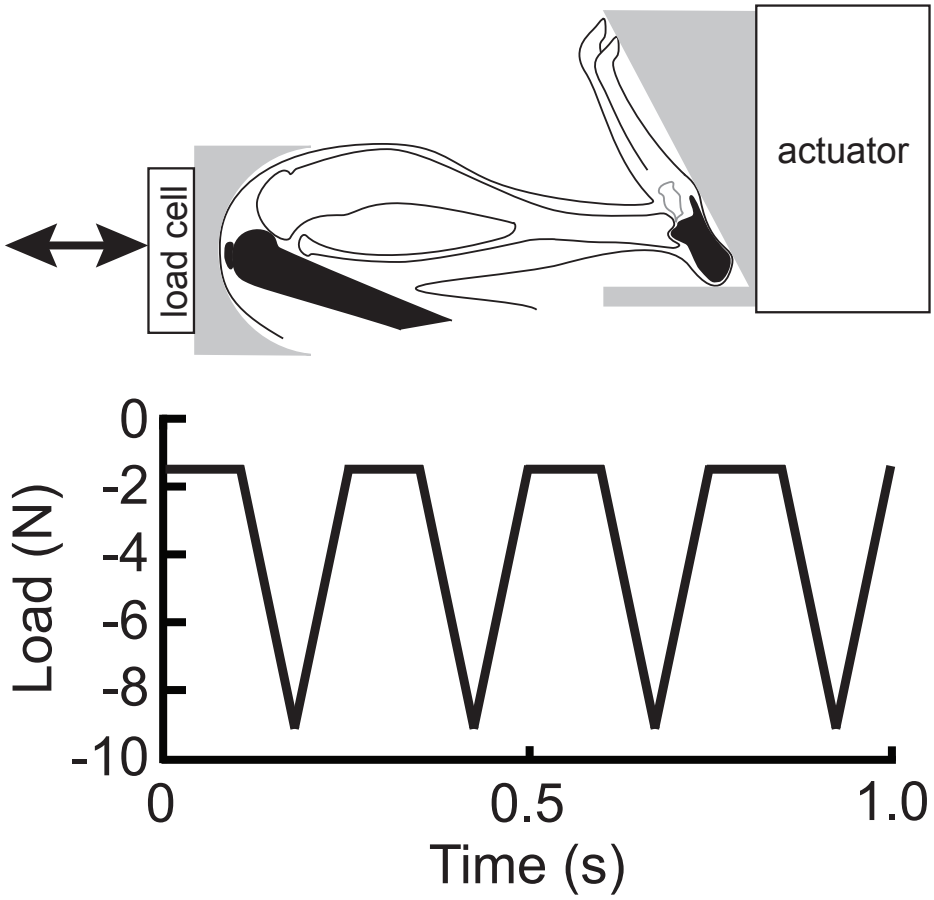

FIGURE 2

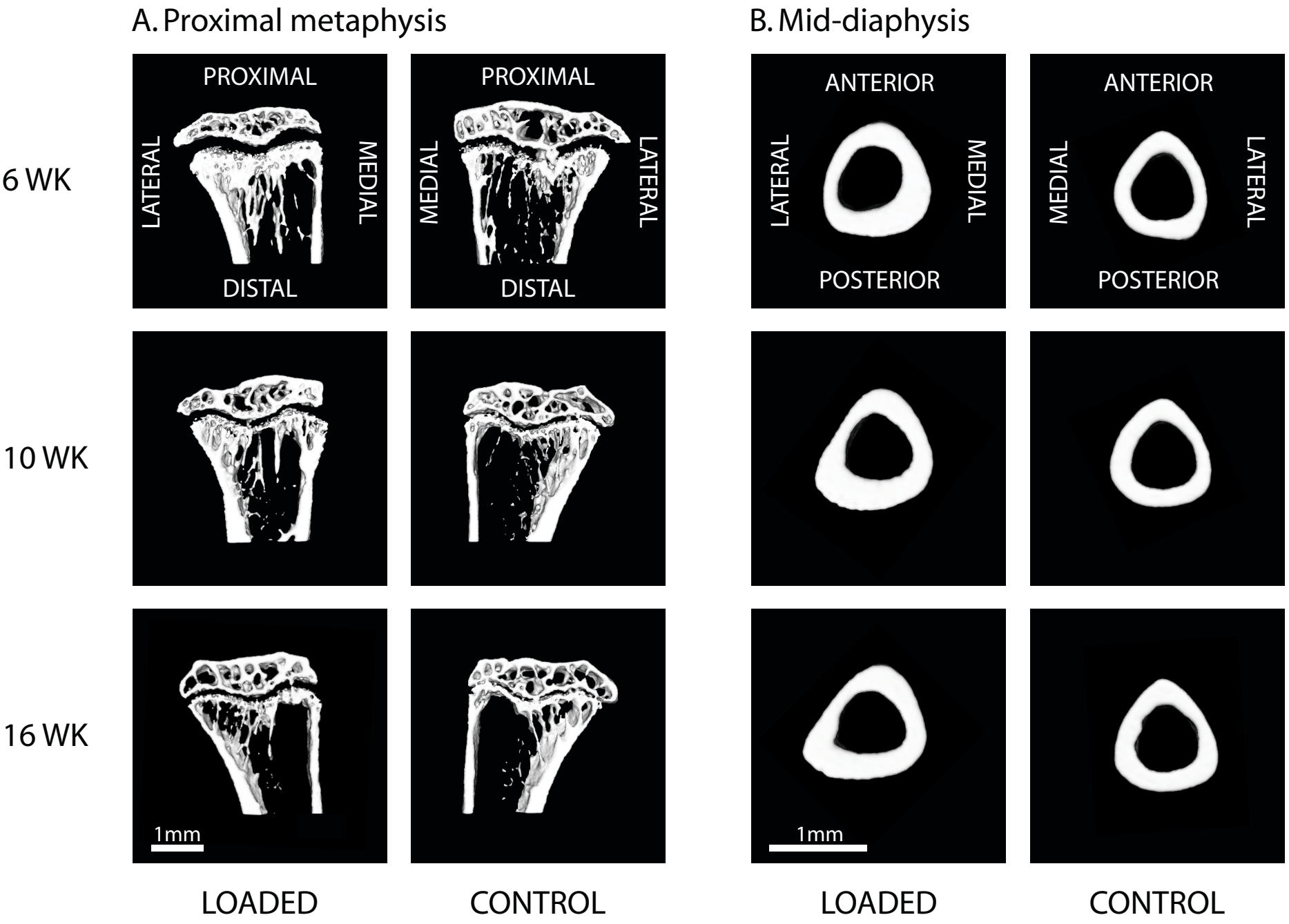

FIGURE 3

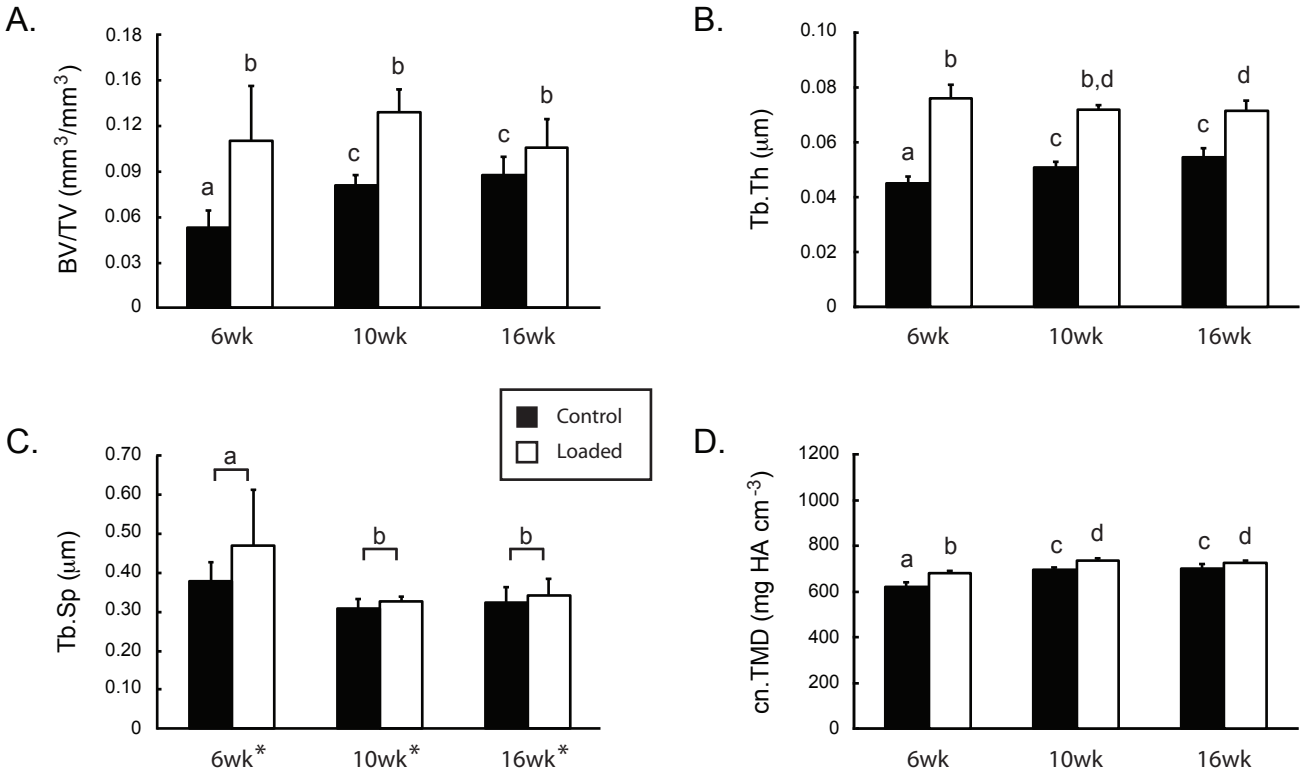

FIGURE 4

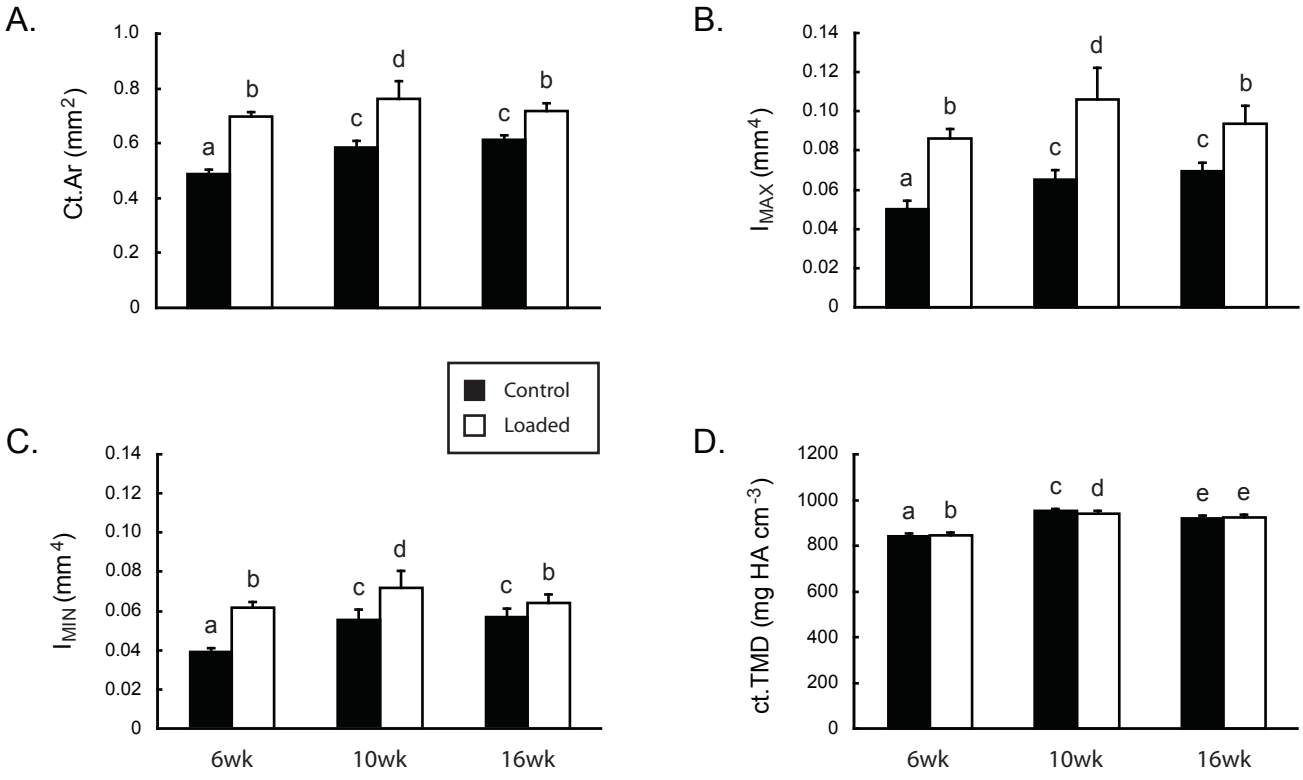

FIGURE 5

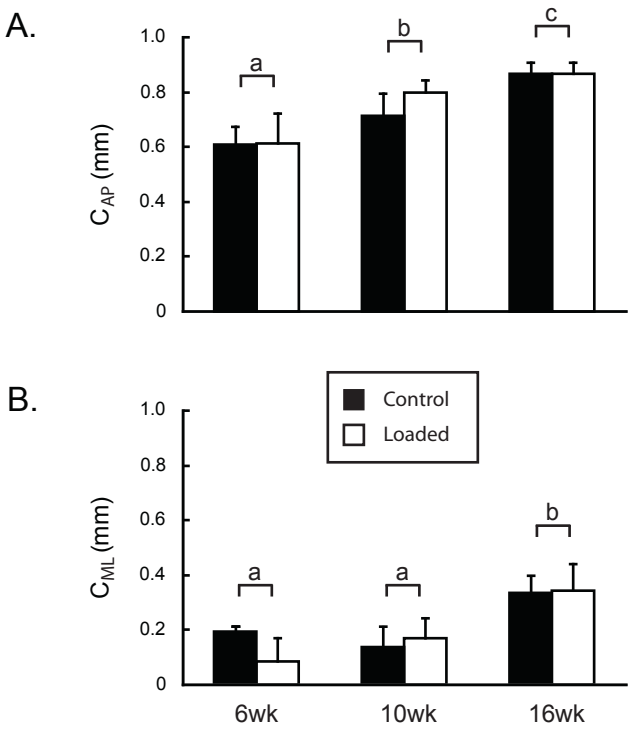

FIGURE 6

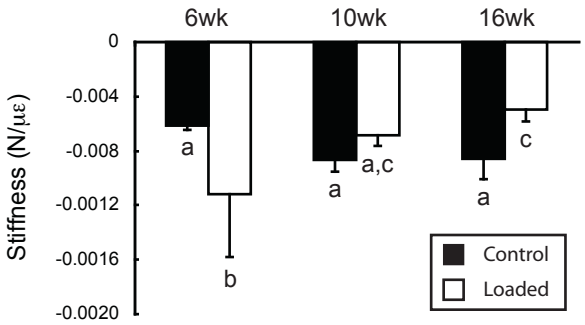

FIGURE 7

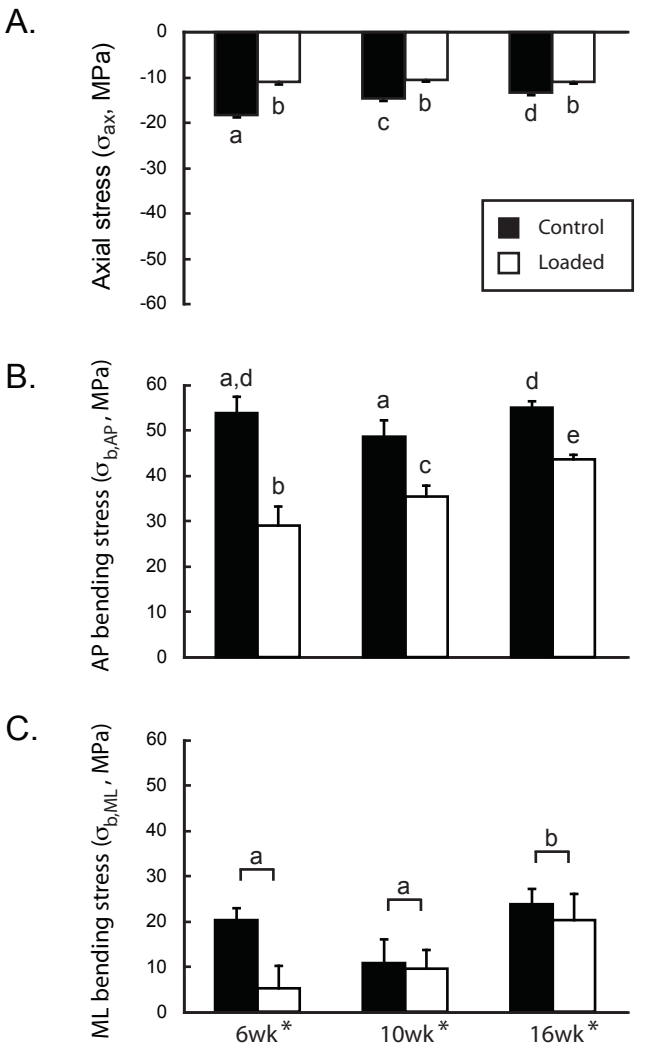

Table 1: Statistical results for the linear mixed models with repeated measures used to test for the effects of age and load and their interaction.

	Main effect p-values		
	Age	Load	Interaction
Cancellous parameters			
BV/TV (mm^3/mm^3)	**0.020**	**<0.001**	**0.002**
Tb.Th (μm)	0.143	**<0.001**	**<0.001**
Tb.Sp (μm)	**0.001**	**0.019**	0.126
cn.TMD (mg HA cm^{-3})	**<0.001**	**<0.001**	**<0.001**
Mid-diaphyseal parameters			
Ct.Ar (mm^2)	**<0.001**	**<0.001**	**<0.001**
I_{MAX} (mm^4)	**<0.001**	**<0.001**	**0.002**
I_{MIN} (mm^4)	**<0.001**	**<0.001**	**<0.001**
ct.TMD (mg HA cm^{-3})	**<0.001**	0.498	**0.002**
Whole bone measures			
C_{AP} (mm)	**<0.001**	0.320	0.455
C_{ML} (mm)	**0.003**	0.488	0.257
Tibial length (mm)	**<0.001**	**0.003**	**0.002**
Stiffness measures and stress analyses			
Stiffness (N/με)	0.225	0.884	**0.003**
σ_{ax} (MPa)	**<0.001**	**<0.001**	**<0.001**
$\sigma_{b,AP}$ (MPa)	**<0.001**	**<0.001**	**0.002**
$\sigma_{b,ML}$ (MPa)	**0.005**	**0.011**	0.051

Bold indicates a significant effect at $p<0.05$. Sample sizes for the cancellous and mid-diaphyseal measures were N=10, 6, and 12 for the 6wk, 10wk, and 16wk old mice, respectively. Sample sizes for the whole bone morphological and stiffness measures and stresses induced by 9N compressive loads were N=3, 3, and 4 for the three age groups.

Table 2: Pair-wise comparisons where the linear mixed model analyses in Table 1 indicated significant age-load interactions in the tibial response to applied load.

	Load effects			Age effects					
				Non-loaded Control (right)			Loaded (left)		
Cancellous parameters									
	6wk	10wk	16wk	6wk-10wk	6wk-16wk	10wk-16wk	6wk-10wk	6wk-16wk	10wk-16wk
BV/TV	**<0.001**	**<0.001**	**0.011**	**0.030**	**0.001**	1.000	0.187	1.000	0.067
Tb.Th	**<0.001**	**<0.001**	**<0.001**	**0.009**	**<0.001**	0.089	0.087	**0.011**	1.000
cn.TMD	**<0.001**	**<0.001**	**<0.001**	**<0.001**	**<0.001**	0.911	**<0.001**	**<0.001**	0.479
Mid-diaphyseal parameters									
Ct.Ar	**<0.001**	**<0.001**	**<0.001**	**<0.001**	**<0.001**	0.184	**<0.001**	0.320	**0.011**
I_{MAX}	**<0.001**	**<0.001**	**<0.001**	**0.001**	**<0.001**	0.816	**<0.001**	0.098	**0.006**
I_{MIN}	**<0.001**	**<0.001**	**<0.001**	**<0.001**	**<0.001**	1.000	**<0.001**	0.720	**0.004**
ct.TMD	**0.048**	**0.003**	0.360	**<0.001**	**<0.001**	**<0.001**	**<0.001**	**<0.001**	**0.005**
Stiffness measures and stress analyses									
Stiffness	**0.007**	0.279	**0.019**	0.421	0.370	1.000	**0.048**	**0.003**	0.664
σ_{ax}	**<0.001**	**<0.001**	**<0.001**	**<0.001**	**<0.001**	**0.002**	0.618	1.000	0.538
$\sigma_{b,AP}$	**<0.001**	**<0.001**	**<0.001**	0.117	1.000	**0.025**	**0.041**	**<0.001**	**0.006**

Bold indicates a significant load or age effect at $p<0.05$.